

Fast and dynamically reliable symplectic integration for solar system N -body problems

David M. Hernandez ^{*}

*Department of Physics and Kavli Institute for Astrophysics and Space Research,
Massachusetts Institute of Technology, 77 Massachusetts Ave., Cambridge, Massachusetts 02139, USA*

12 January 2019

ABSTRACT

We apply one of the exactly symplectic integrators, that we call HB15, of Hernandez & Bertschinger (2015) to solve solar system N -body problems. We compare the method to Wisdom-Holman methods (WH), MERCURY, and others and find HB15 to have high efficiency. Unlike WH, HB15 solved N -body problems exhibiting close encounters with small, acceptable error, although frequent encounters slowed the code. Switching maps like MERCURY change between two methods and are not exactly symplectic. We carry out careful tests on their properties and suggest they must be used with caution. We use different integrators to solve a 3-body problem consisting of a binary planet orbiting a star. For all tested tolerances and time steps, MERCURY unbinds the binary after 0 to 25 years. However, in the solutions of HB15, a time-symmetric Hermite code, and a symplectic Yoshida method, the binary remains bound for > 1000 years. The methods' solutions are qualitatively different, despite small errors in the first integrals in most cases. Several checks suggest the qualitative binary behavior of HB15's solution is correct. The Bulirsch-Stoer and Radau methods in the MERCURY package also unbind the binary before a time of 50 years.

Key words: celestial mechanics - methods: numerical - planets and satellites: dynamical evolution and stability

1 INTRODUCTION

The dynamics of solar systems, star clusters, or galaxies are gravitational N -body problems to first approximation (Heggie & Hut 2003). Gravity determines dynamics on large scales; due to charge screening electromagnetic effects are not relevant at these scales.

Many dynamical problems in science are unified under the Hamiltonian formalism. A Hamiltonian is a C^1 function. For a class of coordinate systems, the N -body Hamiltonian is

$$H(R, P) = \frac{1}{2} P^\dagger M^{-1} P + V(R). \quad (1)$$

R and P are canonical position and momentum vectors respectively, with size $3N$, V is a potential energy, and M is a positive definite mass matrix of size $3N \times 3N$. M is diagonal if we work in a coordinate system where the Hamiltonian is quadratic in the momenta; the coordinates which are simplest for our purposes, such as Jacobi coordinates, Democratic Heliocentric coordinates, or inertial Cartesian

coordinates, satisfy this criteria. In inertial Cartesian coordinates, eq. 1 is

$$H(x, p) = \sum_{i=1}^N \frac{p_i^2}{2m_i} - G \sum_{i=1}^N \sum_{j=i+1}^N \frac{m_i m_j}{|x_i - x_j|} \quad (2)$$

For particle i , x_i and p_i are its phase space coordinates and m_i its mass. G is the gravitational constant. We must solve the coupled system of $6N$ ordinary differential equations resulting from Hamilton's equations:

$$\begin{aligned} \frac{d}{dt} R &= M^{-1} P \\ \frac{d}{dt} P &= F(R), \end{aligned} \quad (3)$$

where $F(R) = -\nabla_R V(R)$.

The solution to equations 3 cannot generally be written as a quadrature for $N > 2$; a practical solution uses numerical integration. But numerical integration is subject to round-off and truncation error, which in general increase secularly. Truncation error is due to the finite order of the method and frequently shows linear error growth in energy or angular momentum. Unbiased rounding error has the same growth in time as Brownian motion; this behavior is

^{*} Email: dmhernan@mit.edu

also known as Brouwer’s law (Brouwer 1937). If t is time, Brouwer’s law says that energy, and other first integral, errors grow as $t^{1/2}$ if the truncation error is smaller than the roundoff error. Biased energy growth is linear in time. Biased growth is avoided by being careful with the chosen numerical integrator (Hairer, McLachlan & Razakarivony 2008; Laskar et al. 2004), by using the number format called Universal Numbers, Unum, (Gustafson 2015) or by other methods.

Geometric integrators (Hairer, Lubich & Wanner 2006) are the method of choice for solving equations 3 for long time scales. One reason is that geometric integrators mitigate secular growth in truncation error. Rather than focus on small errors which may rapidly accumulate, these maps aim to conserve structure of the governing differential equations. They address qualitative questions such as “Will a species survive?” or “Is an orbit stable?” One geometric method is the symplectic method. Symplectic maps preserve all n Poincaré invariants, and the volume of arbitrary regions of phase space. n is the number of degrees of freedom: $n = 3N$ in the N -body case.

Symplectic methods have been developed for special astrophysical N -body problems. One example is the cosmological simulation code **Gadget** (Springel 2005). **Gadget** solves the dark matter N -body problem where relaxation times are long compared to time scales of interest. Nearly regular planetary simulations have been successfully studied with the symplectic method of Wisdom & Holman (1991) (WH), which was further developed by Duncan, Levison & Lee (1998) and others.

N -body problems with a hierarchy of time scales are difficult to study with symplectic methods. Changing the time step in effect produces a time dependent effective Hamiltonian (Sanz-Serna & Calvo 1994) leading, generally, to a secular growth in the magnitude of energy error.

Geometric methods are responsible for important solar system dynamics discoveries. WH was used to show that the orbit of pluto is chaotic (Wisdom & Holman 1991). The original WH (WHJ) uses canonical Jacobi coordinates and momenta. Duncan, Levison & Lee (1998) developed a WH version (WHD) by writing the positions as heliocentric coordinates and the center of mass coordinates. The corresponding canonical momenta are the barycentric momenta and total momentum. This phase space coordinate system is called Democratic Heliocentric Coordinates (DHCs). A feature of WH is that the center of mass degrees phase space coordinates do not enter in the equations of motion of the other phase space coordinates so the center of mass phase space coordinates can be ignored.

The original WH has a limited range of usefulness. WHJ has a greater applicability than WHD. By changing the numbering of the Jacobi coordinates, WHJ accommodates a small degree of complexity in solar systems, such as a binary star. A similar degree of complexity is achieved by the method of Chambers et al. (2002). But WHJ fails for solar systems with multiple stars and planetary moons, or systems with non-stellar close encounters within the Hill radii of the objects. These conditions are common: 40 – 50% of Kepler exoplanet host stars are binary stars (Horch et al. 2014) and triples make up 10% of galactic stellar systems (Antognini & Thompson 2015, and references therein). Planet formation simulations have strong encounters. These

and other facts make WH unsuitable for a wide range of problems.

Switching integrators were developed by Chambers (1999) (called **MERCURY**), Duncan, Levison & Lee (1998) (called **SyMBA**), Kvaerno & Leimkuhler (2000), and others to model systems where WH fails. A switching integrator switches the integration method as a function of phase space coordinates. For example, **MERCURY** reduces to WHD when non-solar objects remain well-separated. Switching integrators are not strictly symplectic because they are not symplectic everywhere in phase space. The switch can also introduce an artificial drift in error and break time reversibility. The dynamics in these integrators could be qualitatively wrong. This is concerning since important dynamics predictions have been derived using switching integrators (Batygin, Brown & Betts (2012), etc). We explore these problems with switching integrators in this paper.

Another solution for systems where WH fails is to use general, or hierarchical, Jacobi coordinates, whose structure changes depending on the problem. Unfortunately, writing a new coordinate system and integrator for each problem is cumbersome. It would be simpler to have one coordinate system and integrator for all solar system N -body problems.

Rein & Spiegel (2015) developed a non-symplectic 15th order integrator and compared its efficiency, the computation time vs the error, with WH. **IAS15** is especially efficient for small energy errors (roughly 10^{-10} or smaller), as was shown by Rein & Spiegel. To understand the significance of small errors we must first discuss the meaning and usefulness of chaotic N -body integrations beyond the integration Lyapunov time. Quinlan & Tremaine (1992) showed that N -body orbits are, at least sometimes, shadowed by a true orbit of the original Hamiltonian with close initial conditions to those used in the N -body integration. The smaller the integration errors in the conserved quantities, the closer the integration initial conditions are to the shadow orbit’s initial conditions. More work is needed to determine how shadow orbits apply to more realistic N -body integrations.

Perhaps a more reliable and practical way to understand N -body integrations for longer than their Lyapunov time is in an averaged sense; the statistics of N -body integrations are assumed to approximate the true statistics of the N -body Hamiltonian solution. The validity of this assumption was recently supported (Portegies Zwart & Boekholt 2014). For integration times longer than the Lyapunov time, a high accuracy solution (roughly 10^{-6} or smaller energy error) may not make sense (Portegies Zwart & Boekholt 2014), but errors should remain bounded; symplectic methods are ideal for this requirement. Therefore, a high order code like **IAS15** may be most useful if both the time scale is shorter than a Lyapunov time and if extreme accuracy is needed, while a lower-order symplectic method may be favored in other cases. Even under the conditions of high accuracy and short times, a low order symplectic is reliable: we note that the errors of a symplectic method are deceptive. The errors can often be reduced to the machine precision level by applying a symplectic corrector (Wisdom, Holman & Touma 1996). The symplectic corrector only needs to be applied at times when accurate output is needed, after the inverse corrector has been applied at time 0. Symplectic correctors add negligible computational cost compared with the integration cost.

Hernandez & Bertschinger (2015) introduced a symplectic and reversible method (hereafter HB15) for N -body problems with small relaxation times. HB15 was tested on simple regular and chaotic N -body problems and the method was found to be efficient against other methods. Its most straightforward use is with inertial Cartesian coordinates; it is not compatible with Jacobi coordinates or DHCs. By construction, it exactly conserves all N -body integrals of motion, except for the energy, to machine precision. It can be shown that a symplectic method cannot be constructed to conserve all integrals exactly (Zhong & Marsden 1988). HB15 typically requires solving a series of two-body problems with elliptic and hyperbolic orbits.

In this paper we apply HB15 to a variety of problems in solar system dynamics. For problems for which WH methods are designed, HB15 has efficiency comparable to WHD, and provides an alternative to WH, with the added benefit of using inertial Cartesian coordinates. For problems where WH fails, HB15 provides efficiency comparable to or better than MERCURY. It is naturally suited for solving problems with a variety of stable hierarchies without having to derive new coordinates and integrators. It is slower for a problem with frequent close encounters, but errors are small regardless of the closeness of the encounter. From a practical standpoint, HB15 is simple to implement. We also compare HB15 against alternatives to switching methods. We use the efficient two-body solver introduced in Wisdom & Hernandez (2015). It solves the two-body problem in universal variables without using the Stumpff series. HB15 follows Brouwer's law like IAS15.

The organization of the paper is as follows. In Section 2 we provide an overview of HB15 and compare it to WH. Numerical solar system comparison tests are carried out in Section 3. Section 4 discusses switching integrators and their pitfalls. Section 5 presents our conclusions and recommendations for numerical methods in solar system calculations.

2 OVERVIEW OF HB15 AND COMPARISON WITH WISDOM-HOLMAN METHOD

We use the N -body problem of the Sun and gas giant planets to compare the steps of HB15 and WHD. Pseudocode for general HB15 is presented in Hernandez & Bertschinger (2015) Section 4, and we restate it here. A drift of time h updates positions by adding a linear term in the momenta. For HB15, a drift to particle i is $x'_i = x_i + hp_i/m_i$. A kick to particle i due to particle j updates i 's momentum. For HB15, $p'_i = p_i + hF_{ij}(x)$ (see eq. 3). The pairs of particles are divided into a kick or Kepler solver group. We place into the Kepler solver group those pairs that are on a nearly Keplerian orbits or that may have a close encounter. For a Sun and gas giants integration, the most efficient choice is that the four planet-sun pairs go in the Kepler group, while the other 6 pairs go to the kick group. The groups cannot change during integration. Doing so would introduce a time dependence in the integrator "Hamiltonian" \tilde{H} (Hernandez & Bertschinger 2015).

With these definitions and instructions, we can define a map ϕ_h , shown in Algorithm 1. We label operators A_h , B_h , and C_h , which will be discussed below eq. 5. Transpose map ϕ_h^\dagger is Algorithm 1 with the steps reversed. Then the order 2

```
(Begin  $C_h$ ) ;
Drift all particles for time  $h$  ;
(Begin  $B_h$ ) ;
for pairs of particles  $(k, l)$  getting kicks do
    Kick particles  $k$  and  $l$  for time  $h$  using their
    mutual force ;
end
(Begin  $A_h$ ) ;
for rest of pairs  $(i, j)$  do
    Drift particles  $i$  and  $j$  for time  $-h$  ;
    Apply a Kepler solver to advance the relative
    coordinates and velocities of  $i$  and  $j$  by  $h$  ;
    Advance center of mass coordinates of  $i$  and  $j$  by
     $h$  assuming their two-body total momentum is
    conserved ;
    Update inertial Cartesian coordinates and
    velocities of  $i$  and  $j$  by using the results of the
    previous two steps ;
end
```

Algorithm 1: Pseudocode for ϕ_h , the building block of HB15.

method of HB15 is given by

$$\phi_h^2 = \phi_{h/2}^\dagger \phi_{h/2}. \quad (4)$$

ϕ_h^2 is twice as computationally expensive as ϕ_h , but it is time reversible. We find time reversible methods perform better than non-reversible ones. Hairer, Lubich & Wanner (2006) shows reversibility can be as advantageous as symplecticity. Second order WH methods in theory and practice are also time reversible. It is unclear how much of their efficiency is due to their symplecticity or reversibility.

If A_h , B_h , and C_h are operators of time step h , both HB15 and WHD are written

$$\phi_h^2 = C_{h/2} B_{h/2} A_{h/2}^\dagger A_{h/2} B_{h/2} C_{h/2}. \quad (5)$$

$C_{h/2}$ is a drift, which is not equivalent for the two methods. Let u and v be the position and momentum in DHCs. Then a drift of particle i gives $u'_i = u_i + h/(2m_i) \sum_{i=2}^N v_i$. $i = 1$ corresponds to the Sun. $B_{h/2}$ is a kick, which is identical for the two methods, and described above. The commutator $[B_h, C_h] = 0$ for WHD and WHJ, meaning the order in which the operators are applied does not change the solution, ignoring roundoff error, but generally $[B_h, C_h] \neq 0$ for HB15. A_h solves Kepler problems exactly.

For WHD there is a simplification in the form of map 5: $A_{h/2}^\dagger A_{h/2} = A_h$. A_h solves Hamiltonian

$$H(u, v) = \sum_{i=2}^5 \left(\frac{v_i^2}{2m_i} - \frac{Gm_i m_1}{|u_i|} \right). \quad (6)$$

These are 4 independent Kepler problems with 3 degrees of freedom each. $H(u, v)$ is solved exactly using a Kepler solver such as that described in Wisdom & Hernandez (2015).

For HB15, $A_h^\dagger \neq A_h$. The computationally expensive part of solving A_h , picked out in Algorithm 1, is integrating using the Hamiltonians

$$H_i(x, p) = \frac{p_i^2}{2m_i} + \frac{p_1^2}{2m_1} - \frac{Gm_i m_1}{|x_i - x_1|}, \quad (7)$$

for $i > 1$. The $H_i(x, p)$ each have analytic solutions, but

the order in which the $H_i(x, p)$ are solved changes the general solution. Applying $A_{h/2}^\dagger A_{h/2}$ implies solving $H_i(x, p)$ in a given order and then in reverse order ensuring time reversibility. Hernandez & Bertschinger (2015) found that the time-reversible method ϕ_h^2 performed better than ϕ_h , even though they are both second order accurate.

Since $A_h^\dagger \neq A_h$ for HB15, HB15 uses twice as many Kepler solvers as WH, making HB15 more computationally expensive. We now explore the computation times of the two methods. HB15 found a Kepler solver was $\approx 40\%$ more computationally expensive than a kick, but this rough figure will vary depending on the Kepler solver, the orbit, the time step, the programming language, and so forth. A drift had negligible impact on computational resources. If n pairs are put in the Kepler solver group, and t_0 is the cost of a kick, HB15's cost for one time step is approximately

$$t = \left(\frac{N(N-1)}{2} - n + 1.4(2n) \right) t_0. \quad (8)$$

$N = 4$ for the gas giants problem. WH's cost is less: we replace the $2n$ by n . Therefore, for a Sun and gas giants problem we expect HB15 to be $\approx 48\%$ slower than WHD. We expect a smaller difference with WHJ since WHJ's kick step is more expensive. In practice HB15's method is only 6–10% slower than the implementation of WHD in MERCURY.

We explore factors responsible for HB15's faster than expected performance. First is the Kepler solver, described in Wisdom & Hernandez (2015). A Kepler solver test for elliptical orbits was nearly twice as fast as a C version of the solver in MERCURY, which we call `drift_one.c`. For hyperbolic orbits, `drift_one.c` was 60% slower. HB15 is written in C and we used compiler optimizing option `gcc -O3`. MERCURY was written in Fortran, which can be faster or slower than C. MERCURY was run without output in this and all other efficiency tests in this paper to make it as fast as possible. MERCURY was compiled with `gfortran`, following MERCURY instructions.

These and other tests described later indicate HB15 can be an alternative to WH. As the number of planets increases, the timing difference between HB15 and WH becomes smaller as kicks dominate computation time. A benefit of HB15 is that it restores the problem's center of mass degrees of freedom and conserves them exactly, making it easy to follow motion in arbitrary inertial frames. The error in the center of mass is given by roundoff error which is smallest if working in a center of mass frame, and is found to follow Brouwer's law, as we will see in Section 3.2.

Ignoring roundoff and Kepler solver error, HB15 solves the two body problem exactly. We can check analytically that WHD does not. This fact was also pointed out by Wisdom (2006). We can test this using MERCURY's WHD. We integrate a Jupiter mass planet at 1 AU in circular orbit around a solar mass star for one time step $h = 10$ years and we get $|\Delta E/E| = 8.9 \times 10^{-11}$, more than five orders of magnitude larger than machine precision. HB15's solution that results from integrating the same problem for the same h has $|\Delta E/E| = 1.1 \times 10^{-16}$, the machine precision.

It will be useful for later to discuss the conservation of angular momentum when applying WHJ. As shown in Hernandez & Bertschinger (2015), HB15 conserves angular momentum exactly. WHJ has analogous operators A_h , B_h , and C_h of eq. 5 (Rein & Tamayo 2015). Let the angular mo-

mentum operator be D_L . Let a and b be a canonical set of Jacobi coordinates. With i a particle number, the angular momentum vector satisfies $L = \sum_i x_i \times p_i = \sum_i a_i \times b_i$. Then it is straightforward to show that $[D_L, A_h] = [D_L, B_h] = [D_L, C_h] = 0$. The implication is that WHJ conserves angular momentum exactly. Symplectic correctors, also composed of A_h , B_h , and C_h , do not affect the angular momentum conservation.

3 COMPARISON TESTS OF METHODS

3.1 Hierarchical Triples

Most solar systems probably have at least one hierarchical triple. One example is a planet orbiting a binary star. A planet-moon configuration orbiting a star is another hierarchical triple.

These systems are quasi-periodic, meaning the Kolmogorov-Arnold-Moser (KAM) theorem can apply. The KAM theorem says that if a sufficiently differentiable map is perturbed from an integrable problem, invariant curves persist if the perturbation is small and the rotation number is not close to a rational number. A symplectic map is especially suited for such a problem in long term dynamics of billions or more orbits. First we study the hierarchical triple system with parameters described in Duncan, Levison & Lee (1998). A binary planet system has semi-major axis $a = 0.0125$ AU and eccentricity $e = 0.6$. Its center of mass is in a circular orbit at 1 AU from a solar mass star. The planets have Jupiter masses. The motion is constrained to a plane.

We apply different methods to evolve this system: HB15, MERCURY (Chambers 1999), and other methods in the MERCURY software package. The other methods are Bulirsch-Stoer (BS), a faster conservative Bulirsch-Stoer, Radau, and WHJ with symplectic correctors and a default Jacobi numbering. The default numbering gives the star the first coordinate. Although we do not use IAS15 we do use a Radau method upon which it is based. The three pairs of particles are placed in the Kepler solver group in HB15. One pair describes elliptic motion while we found the other two always describe hyperbolic motion. We run the problem for 100,000 years, which corresponds to 2.3 billion orbits of the binary. We vary the time step or tolerances in the methods and measure the efficiency in calculating the energy and angular momentum. The errors are output by the MERCURY software and we copy them directly. Results are shown in Fig. 1.

All methods give the qualitatively correct answer that the tight binary remains bound. The slope of the least squares linear fit of the HB15 points is -3.9 . It is nearly twice that expected for a second order method assuming cpu time is inversely proportional to the time step. HB15 is the most computationally efficient method for the given range of energy errors. At smaller errors, HB15 loses its efficiency, as expected, since it is a low order integrator. But the loss of efficiency is deceptive (Section 1): a symplectic corrector could reduce errors dramatically. We expect the slopes of linear fits to MERCURY (which uses BS), BS, and BS2 points to be significantly steeper than the HB15 fit slope, and the data are consistent with this prediction. We can follow the steps in Hernandez & Bertschinger (2015) to construct higher order symplectic integrators, but do not find it necessary due

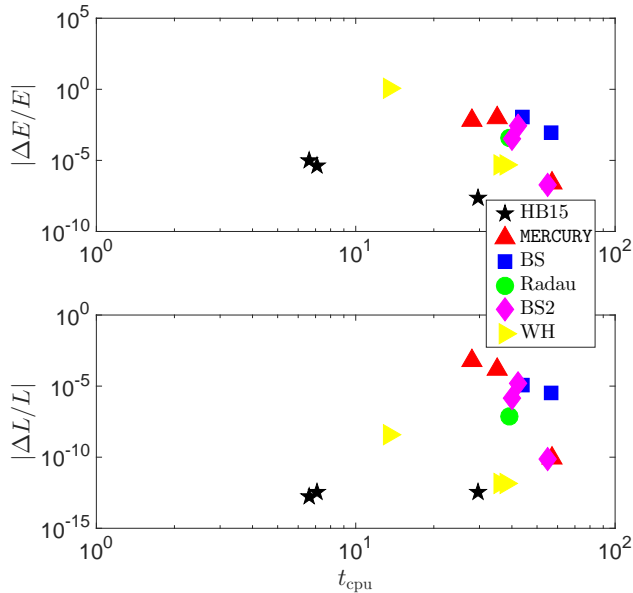


Figure 1. Efficiency for several solar system integrators when solving the binary planet hierarchical triple system problem. The problem is run for 100,000 years. HB15 is most efficient in the range plotted.

to arguments in Section 1. The critical radius for **MERCURY** (Chambers 1999) is set at the default $r_{\text{crit}} = 3r_{\text{Hill}}$.

We note that the error in angular momentum for WHJ (labeled as WH) is a bit large given our predictions in Section 2. This large error was also observed in Rein & Spiegel (2015), Fig. 4, although they did point out it was unexpected. We posit the WHJ implementation of **MERCURY** may have a bug.

We see qualitatively similar results when we test a binary star orbited by a planet. We let the binary stars have $a = 1$ AU. The planet is set at $a = 20$ AU from the center of mass and orbits the center of mass with $e = 0.6$. All motion occurs in a plane. The stars have solar mass while the planet has a Jupiter mass. We run the problem for 10,000 years, which is 10,000 orbital periods of the binary; far fewer than in the previous problem. The results are shown in Fig. 2. In this case, WHJ is as efficient as HB15. Note that WHJ has symplectic correctors applied which reduce its errors. Symplectic correctors applied to HB15 would remove terms in its \tilde{H} and reduce its error. We leave development of symplectic correctors for HB15 for future work.

3.2 The Outer Giant Planets

We began discussion of the problem of the Sun and outer gas giant planets in Section 2. WH uses 4 Kepler solvers per step. HB15 uses 8, but only shows 6–10% slower speed than the **MERCURY** WHD implementation. We place the planet-sun pairs in the Kepler solver group to obtain the most efficient solutions.

We integrate the outer gas giants for 100,000 years for different time steps. To use the WHD method, we ran **MERCURY** with its r_{crit} parameter set to 0. Initial conditions were taken from Hairer, Lubich & Wanner (2006). The effi-

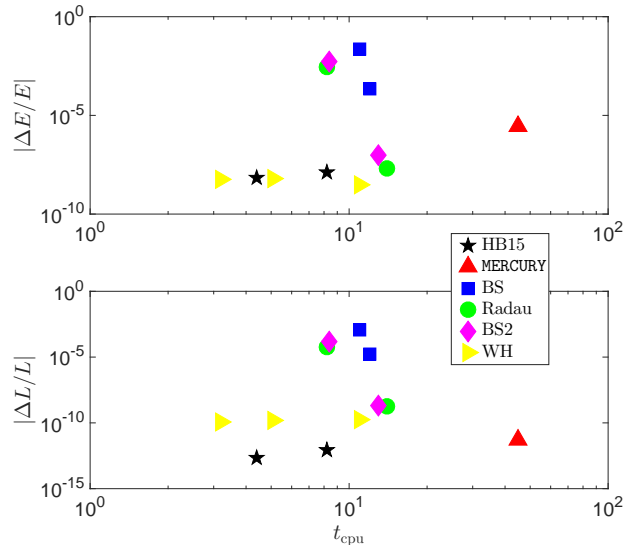


Figure 2. Efficiency, as in Fig. 1 for the solution of a hierarchical triple problem consisting of a binary star orbited by a planet. HB15 and WHJ, with symplectic correctors, are best suited for this problem in the range plotted.

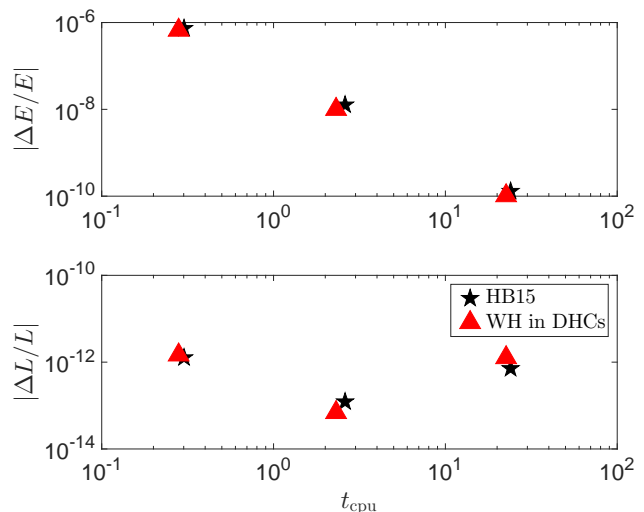


Figure 3. Efficiency plot for the the solution of outer giant planet N -body problem. The problem is run for 100,000 years. HB15 and WHD have similar efficiency.

ciencies of the solutions are shown in Fig. 3. The efficiency of the two methods is similar. The slope in the energy plot is -2 , which is what we expect for second order methods if $t_{\text{cpu}} \sim h^{-1}$. HB15 should show non-secular growth in energy and machine precision accuracy in the other integrals of motion. We check this by calculating the error in conserved quantities when $h = 0.1$ years. The result is shown in Fig. 4. The L_i , p_i , and x_i are the three components of angular momentum, linear momentum, and center of mass position constant, respectively. In this Section, we have shifted to an inertial frame where the initial p_i and x_i are 0, although the shift is not required for HB15 to work well. We see the expected behavior of symplectic and reversible methods. The

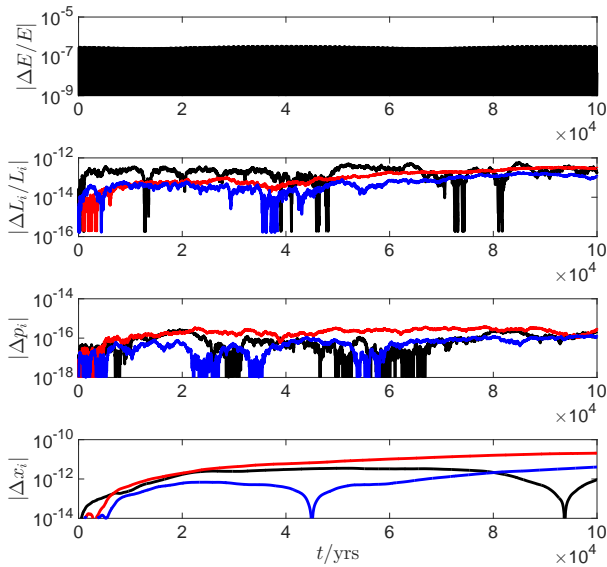


Figure 4. Error in conserved quantities as a function of time for HB15 applied to the outer giants problem. $h = 0.1$ years. We see the expected bounded energy error and machine precision error in other conserved quantities (ignoring roundoff error).

negative dips in the bottom three panels indicate changes of sign. The growth in error in the integrals besides energy is due to roundoff error. Before we examine the growth of roundoff error in Fig. 4, a discussion on biased and unbiased roundoff error growth is in order.

A number of problems cause biased error growth. One example is when numerical constants in the numerical integrator are not defined precisely. Most numerical constants do not have an exact machine representation and a computer uses a rounded approximation to the constant. Also, implicit numerical methods, like IAS15, that use an iterative scheme to find a solution show biased energy growth if the iterative scheme is not done with care. Numerical tricks can be employed to control biased energy error. IAS15 is claimed to achieve Brouwer’s law by being careful with the computer architecture and compiler and using adaptive time steps. Although they do not claim it, they also potentially avoid bias by using accurate coefficients in their method (Hairer, McLachlan & Razakarivony 2008). Fortunately, achieving Brouwer’s law is easy for some numerical methods such as symplectic compositional numerical methods (Hairer, McLachlan & Razakarivony 2008), like HB15, as we will see.

Brouwer’s law means the growth in energy error is a random walk with mean zero and variance proportional to the roundoff unit. For compositional symplectic methods, Brouwer’s law is achieved for other conserved quantities of the symplectic method if they are near the conserved quantities of the continuous problem. This is the case for angular momentum and linear momentum in HB15. In Fig. 4, the growth in time of these quantities is $\approx t^{0.2}$ and $\approx t^{0.5}$ meaning Brouwer’s law is approximately achieved. The center of mass position is expected to grow as $t^{3/2}$ because it is an integral of the linear momenta over time. In agreement with

this expectation, the center of mass position error in Fig. 4 grows as $\approx t^{1.3}$. Our results agree with those of Laskar et al. (2004), who performed full solar system integrations without any special provisions for roundoff error, using a symplectic composition method, and also achieved Brouwer’s law. WHJ was found to be biased in Rein & Spiegel (2015). One reason it may be biased could be the Kepler solver it uses, *drift_one*, which is biased (Wisdom & Hernandez 2015). Note that MERCURY, as we will see in Section 4.3, is not exactly a composition method, and will not necessarily have the roundoff advantage of composition methods.

Rein & Spiegel (2015) also discussed ways of reducing the random Brouwer’s law error. Roundoff error is noticeable if it is at the level of truncation error, which is typical of a high order method like IAS15.

Fig. 4 is a similar test to that which was done in Duncan, Levison & Lee (1998) to test WHD. The error in energy is bounded and remains bounded for larger h . HB15 should be symplectic and show favorable long term energy conservation regardless of what pairs are put in the Kepler group in Algorithm 1. If we put all pairs in the solver group, HB15 is unnecessarily slow. Using eq. 8 with $N = 5$, and $n = 4$ and $n = 10$, we find using all pairs should be 60% slower. In practice we find using all pairs is twice as slow. With all pairs in the Kepler solver group of Algorithm 1, we again choose $h = 0.1$ years and we find expected error behavior similar to that in Fig. 4 (not shown here).

3.3 The Outer Gas Giants with a Binary Planet

We increase the complexity of our tests by combining the binary planet problem from Section 3.1 and the outer giant planets problem from Section 3.2; the particles are the Sun and 6 total planets. The same pairs are left in the Kepler solver group: there are 21 pairs, 8 solved with Kepler solvers. WH breaks down for this problem and we must use MERCURY or a similar method for comparison. We choose MERCURY because it is frequently used to solve a variety of solar system problems in the literature.

We tried other complex problems such as the outer gas giants plus Pluto and Charon or the outer gas giants plus the Earth and Moon. The qualitative efficiency results were not different. We run the problem for 1000 years, which is $\approx 23,000$ orbits of the binary. Efficiency plots are shown in Fig. 5.

The efficiency of the two methods varies. HB15 is most efficient for fast computations, as expected. MERCURY shows a steeper slope and eventually at the smallest errors becomes most efficient. The slopes of a least squares linear fit to the points are -16 and -3.8 . The slope of HB15 is nearly twice as large as expected again.

3.4 The Massive Outer Gas Giants

We tested a massive outer solar system, where the planet masses are increased by a factor 50. This problem was studied in Duncan, Levison & Lee (1998) and Chambers (1999). The problem is chaotic and it is not useful to look at one set of initial conditions. The chaos is due to the numerical method and the continuous physical Hamiltonian. Because of numerical chaos that depends on the method, it is difficult to compare methods for this problem.

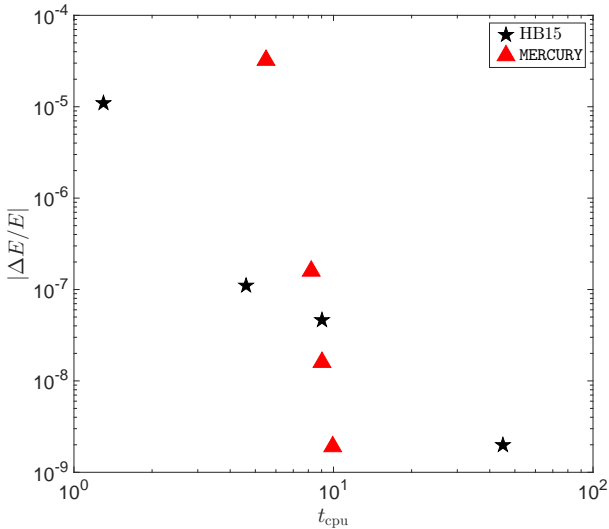


Figure 5. Efficiency of MERCURY and HB15 for the solution of the outer gas giants with a binary planet problem. The problem is run for 1000 years. HB15 is most efficient at larger error ranges.

To measure chaos, we calculate the growth in the L_1 norm, which is a measure of phase space distance. For $h = 0.001$ years, during the first 100 years, the growth in the norm was between linear and quadratic, a growth characteristic of regular problems. For $h = 0.005$ years, during the same time period, the growth was exponential with Lyapunov time scale of about 40 years.

We run the problem with different time steps and different initial conditions. New initial conditions are obtained by perturbing a phase space coordinate by 1×10^{-14} . We run the problem for 3000 years, as is done in Duncan, Levison & Lee (1998). Close encounters can occur between any pairs so we place all pairs in the Kepler solver group of Algorithm 1. With all pairs in the Kepler solver group, HB15 will compute at its slowest (see eq. 8 with $n = N(N - 1)/2$, n 's maximum value).

In Fig. 6 we plot the error at the end of 3000 years as a function of the closest encounter during the run. The closest encounter is in units of Jupiter's Hill radius, which is 1.15 AU at time 0. Jupiter's Hill radius is of equal or smaller magnitude than the other planets' Hill radii. The three colors correspond to $h = 0.001$, $h = 0.005$, and $h = 0.01$ years, with approximate computation times of 30, 6, and 3 seconds, respectively. The errors in all runs are satisfactory. The slope of a linear fit to the purple points is ≈ -3 , and the slope of a linear fit to the blue points is ≈ -1.8 . So for smaller time steps, the energy errors grow the most when we change the closest approach distance. The closest encounter in the plot was $r_{\text{close}} = 0.0087$ AU, which is comparable to that reported by Chambers (1999), as is the energy error. It has been reported that the method of Duncan, Levison & Lee (1998) fails for close enough encounters (Kvaerno & Leimkuhler 2000).

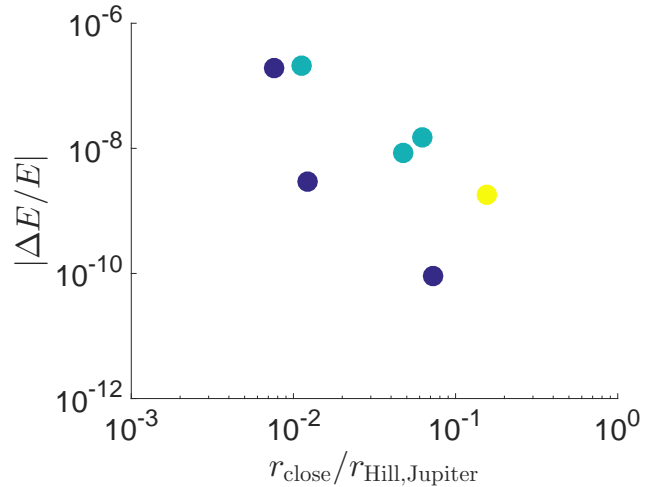


Figure 6. Energy error as a function of the closest approach for the solution of the massive outer gas giants problem. A solution is obtained for the first 3000 years using HB15. The three colors correspond to $h = 0.001$, $h = 0.005$, and $h = 0.01$ years, with approximate computation times of 30, 6, and 3 seconds, respectively. Different points with the same color are different initial conditions.

4 LIMITATIONS OF MERCURY AND SWITCHING INTEGRATORS

4.1 Switching Integrators for the N -body problem

Authors that have solved the N -body problem with switching integrators include Chambers (1999), Duncan, Levison & Lee (1998), Oshino, Funato & Makino (2011), Iwasawa, Portegies Zwart & Makino (2015), and Kvaerno & Leimkuhler (2000). The common strategy is to switch the method when a pair of particles comes in close proximity.

Kvaerno & Leimkuhler studied the effect of the smoothness of the switch in a short timescale problem: 32 orbits of a two-body problem. Their integrator switches between two different symplectic methods. The switch can occur gradually or suddenly: the transition is quantified by a smoothing function. The integrator takes constant time steps. For the C^0 function, a theta step function $\theta(r)$, with r the particle pair separation, the switch occurs at different phases along the orbit, once the integrator realizes it is in a new method region. The C^0 function caused clear secular growth in energy error. As the smoothness was increased from C^0 to C^8 , the secular growth was gradually mitigated, but presumably would be apparent in a long term integration over billions of orbits often necessary in solar system dynamics. They also found deterioration in time reversibility due to the switches.

Symplectic maps have an associated function \tilde{H} , which is an integral when it converges (Dragt & Finn 1976). Thus, it is analogous to a Hamiltonian. \tilde{H} is time independent if the time step is not varied. To understand the effects of switching integrators, we discuss \tilde{H} further using the Standard Map (Lichtenberg & Leiberman 1983), a problem with two canonical variables, x and p , as an example. With K

positive, the Standard Map is

$$\begin{aligned} p' &= p + \frac{K}{2\pi} \sin(x) \\ x' &= x + p'. \end{aligned} \quad (9)$$

x and p are mapped to x' and p' . The question is what is the continuous-time Hamiltonian corresponding to eq. 9. There are two possible answers. The Standard Map is closely related to the one degree of freedom simple pendulum problem with Hamiltonian

$$H(x, p) = \frac{p^2}{2} + \frac{K}{2\pi} \cos(x), \quad (10)$$

which is integrable and non-chaotic. For the first answer, add a time dependence to equation 10, $H_1 = K/(2\pi) \sum_{n \neq 0} \cos(x - n\Omega t)$. Ω is a positive constant and n an integer. Using an identity for Dirac delta functions, we get as the sum $H + H_1$ a new time dependent Hamiltonian

$$H_\delta(x, p, t) = \frac{p^2}{2} + \frac{K}{2\pi} \cos(x) \sum_n \delta(\Omega t - 2\pi n). \quad (11)$$

Chirikov (1979) first wrote down eq. 11. Let $\Omega = 2\pi$. Then solving Hamilton's equations for H_δ starting from $t = 0$ and integrating to $t = 1$ leads to map 9. Thus the first Hamiltonian corresponding to map 9 is the time dependent H_δ . H_δ will not be useful for our purposes.

The second answer is a result of an approximation to solving Hamiltonian 10. Map 9 also results from applying a time independent Hamiltonian \tilde{H} for time h (Hairer, Lubich & Wanner 2006):

$$\begin{aligned} \tilde{H}(x, p) &= H(x, p) - \frac{hK}{2\pi} p \sin(x) + \frac{h^2 K}{24\pi} \left(\frac{K}{2\pi} \sin^2(x) - p^2 \cos(x) \right) \\ &+ \mathcal{O}(h^3). \end{aligned} \quad (12)$$

\tilde{H} arises from applying symplectic Euler to Hamiltonian 10. It can be derived following Hernandez & Bertschinger (2015). When we let $h = 1$, we recover eq. 9. For K small p is bounded, and we find the phase space is constrained by contours of \tilde{H} written to third order in h , a result also found by Yoshida (1993). We do not expect \tilde{H} to converge for chaotic orbits because the orbits do not have an isolating integral. The solutions of applying \tilde{H} and H_δ coincide, if $\Omega = 2\pi/h$, at time $t = h$. We focus on the effect of a switching integrator on \tilde{H} , because it is independent of a continuous time variable.

4.2 A Switch in the Simple Harmonic Oscillator

We focus on an integrable, one-degree of freedom problem, the simple harmonic oscillator. We use it because of its simple regular behavior. The Hamiltonian is

$$H(x, p) = \frac{p^2 + x^2}{2}. \quad (13)$$

The period P of the motion described by H is 2π . Let $y(t)$ be the phase space vector (x, p) at time t . An exact solution for $y(t)$ is found from

$$y(t) = \exp(tD_H)y(0). \quad (14)$$

The operator D_H is defined by $D_H y(t) = \{y(t), H\}$, where $\{\}$ are Poisson brackets. Now we create a switching method

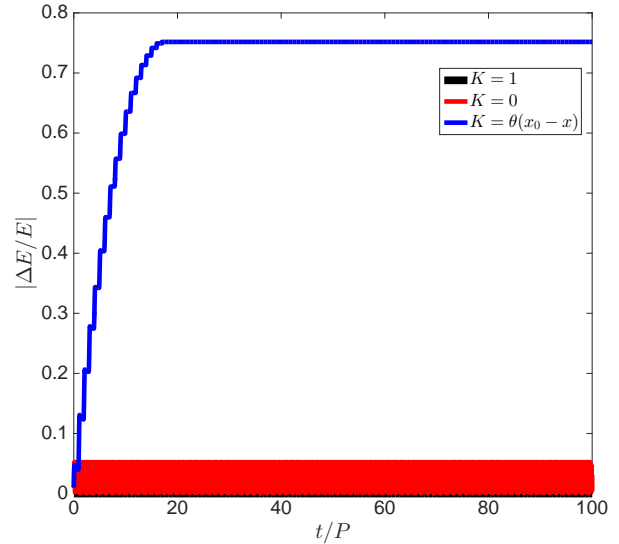


Figure 7. Energy error as a function of time for the solution of the SHO problem. We use a switching method with $h = 0.1$ to obtain the solution. We plot the $K = 0$, $K = 1$, and $K = K(x)$ solutions. The $K = 1$ solution hugs the x -axis. The $K = K(x)$ method shows a secular increase in error due to time dependence introduced into $\tilde{H}_{\text{switch}}$.

to solve eq. 13. Because eq. 13 is integrable, there is no need to construct a switching method to solve it, but doing so will reveal useful properties of switching integrators. Rewrite eq. 13 as $H = H_1 + H_2$ with $H_1 = (p^2 + x^2 K(x))/2$ and $H_2 = x^2(1 - K(x))/2$. Then an approximation to $y(t)$ is

$$\tilde{y}(t) = \exp(tD_{H_1}) \exp(tD_{H_2})y(0). \quad (15)$$

For $K = 0$, eq. 15 gives the symplectic Euler solution. If we choose $t = h < 1$ and iterate eq. 15 with $K = 0$, the solution trajectory satisfies the equation of an ellipse with eccentricity $e < 1$, $Ap^2 + Bpx + Cx^2 - 1 = 0$, with A , B , and C positive numbers. $A = A(h, \tilde{H}_{\text{SO}})$, $B = B(h)$, and $C = C(h, \tilde{H}_{\text{SO}})$, where \tilde{H}_{SO} is the function analogous to eq. 12 for the Hamiltonian of eq. 13. As $h \rightarrow 0$, $e \rightarrow 0$. For $K = 1$, iterating eq. 15 yields the circular $e = 0$ solution trajectory of the Hamiltonian of eq. 13. If $h \rightarrow 0$ for the $K = 0$ trajectory, the two $K = 1$ and $K = 0$ solution trajectories coincide.

As a simple example, let K be a C^0 function, $K(x) = \theta(x_0 - x)$: $K(x)$ is either 0 or 1. We choose $p(0) = 0$, $x(0) = 1$, and $x_0 = 0.5$. The $K = 1$ solution in the x - p plane describes a circle of radius 1. We run the problem for $100P$. We use a step size $h = 0.1$ so there are ≈ 63 steps per period. We plot the error in the energy as a function of time in Fig. 7. We also plot the $K = 1$ solution (it is hugging the x -axis) and the $K = 0$ solution. We see that the $K = 1$ and $K = 0$ solutions have no secular drift in error, except for roundoff error. The growth of energy error for the $K = 1$ solution, not visible in Fig. 7, is linear in time: this t^1 dependence of the error is larger than the $t^{1/2}$ growth described by Brouwer's law.

For $K = \theta(x_0 - x)$ there is a severe and complex growth in error. The growth appears to stop shortly before $t/P = 20$. The explanation for this behavior is as fol-

lows. As t increases, H and \tilde{H}_{SO} increase by a factor 2 or more as the maximum $|p|$ and $|x|$ increase. The difference between H and \tilde{H}_{SO} becomes smaller than the difference of either of them with the initial energy and the growth of the blue curve diminishes. If we reduce h , the growth asymptotes at large t . For larger h , the growth asymptotes at smaller t . We tried higher order switches and different x_0 values and our results are consistent with the results of Kvaerno & Leimkuhler (2000).

We can write $\tilde{H}_{\text{switch}}$ for the solution of eq. 15 by casting eq. 15 into the form

$$\tilde{y}(h) = \exp(hD_{\tilde{H}_{\text{switch}}})y(0). \quad (16)$$

$\tilde{H}_{\text{switch}}$ is then (for more details in the derivation, see Hernandez & Bertschinger (2015))

$$\tilde{H}_{\text{switch}}(x, p) = \frac{p^2 + x^2}{2} + h \left(-xp + \frac{\theta(x - x_0)p}{2} + \frac{\delta(x - x_0)x^2p}{2} \right) + \mathcal{O}(h^2). \quad (17)$$

The discontinuities in phase space coordinate derivatives of $\tilde{H}_{\text{switch}}$ are responsible for the break in symplecticity of the harmonic oscillator switch. As expected $\tilde{H}_{\text{switch}}$ is time independent, which seems to contradict the secular growth in error observed in Fig. 7. The solution to this apparent contradiction is that we introduced time dependence through the behavior at coordinates x near x_0 . Because in practice we switch at x different from x_0 , within $\approx h/(2\pi)$ of x_0 , we are changing the integrator as a function of time, and we are making $\tilde{H}_{\text{switch}}$ time dependent. A similar effect with the **MERCURY** solution was undetectable in our tests. This may be due to the high smoothness of the smoothing function (Kvaerno & Leimkuhler 2000). **MERCURY** introduces additional time dependence to its \tilde{H} because its r_{crit} is a function of time, and the smoothing function is a function of r_{crit} . Any symplectic switching method that does not carefully solve boundary behavior in the switch will suffer from time dependence in its \tilde{H} , possibly causing detectable secular energy error growth in time.

4.3 Symplecticity of MERCURY

Switching integrators that switch between two symplectic methods are not symplectic. The integrator is not symplectic at the phase space points where the smoothing function joins the two methods. \tilde{H} has discontinuities at these phase space points because we cannot practically construct a C^∞ function that is infinitely differentiable. An example of a discontinuous \tilde{H} is shown by eq. 17.

Nonetheless, the problem points are rare and we expect nearby initial conditions to preserve the Poincaré invariants when mapped by **MERCURY**. We can test this. We can calculate symplecticity by testing the $6N \times 6N$ equations in the symplectic condition (Sussman & Wisdom 2001),

$$\Omega = J^\dagger \Omega J. \quad (18)$$

Ω is a constant matrix if we work in a canonical coordinate system. Its form depends on the ordered basis. For ordered basis (x, p) , Ω is

$$\Omega = \begin{bmatrix} 0 & I \\ -I & 0 \end{bmatrix}. \quad (19)$$

Table 1. Measure of symplecticity dR for the solutions of the binary planet hierarchical triple problem. Various integrators are used with displaced initial conditions and $h = 0.001$ years to obtain solutions. Also in the table is the typical error in energy for the initial conditions used in calculating dR . The three formally symplectic methods, WHJ, HB15, and DKD leapfrog, have the lowest dR .

Method	dR	$ \Delta E/E $
WHJ	5.2×10^{-10}	1×10^{-7}
BS	8.6×10^{-10}	3×10^{-16}
Radau	5.6×10^{-10}	1×10^{-16}
HB15	8.8×10^{-11}	3×10^{-10}
DKD Leapfrog	3.9×10^{-11}	4×10^{-7}
SAKURA	1.1×10^{-9}	1×10^{-4}
RK4	2.2×10^{-6}	3×10^{-10}

I is the $3N \times 3N$ identity matrix. J is the Jacobian of the map, and J^\dagger its transpose. Eq. 18 is satisfied if and only if the method is symplectic.

We take one time step of length $h = 0.001$ years in the binary planet problem of Section 3.1. $h = 0.001$ years is 3% of the binary planet orbital period. We calculate dR , which is the sum of all elements in the remainder matrix $R = |J^\dagger \Omega J - \Omega|$. For a symplectic method dR should be 0 to numerical error. It doesn't make sense to sum the elements of R since the elements have different units, but our answer for dR did not change much if we sum the elements of R in a unitless way.

We compute Jacobian elements by calculating 8th order finite differences as a proxy for partial derivatives. We test our calculation of dR on various well known methods. In Table 1 we record the values of dR and the typical energy error for the close initial conditions used in calculating dR .

We test three integrators in the **MERCURY** software package: WHJ with symplectic correctors, BS, and Radau. WHJ is the only strictly symplectic method, but BS and Radau behave almost as well as a symplectic integrator. The result for Radau is consistent with the claims of Rein & Spiegel (2015). The small dR is also reasonable for BS as BS is highly accurate. We show dR for four other integrators not part of the **MERCURY** software: symplectic methods HB15 and Drift-Kick-Drift (DKD) leapfrog (Hernandez & Bertschinger 2015), and non-symplectic methods **SAKURA** (Gonçalves Ferrari, Boekholt & Portegies Zwart 2014) and 4th order Runge-Kutta (RK4). The non-symplectic methods **SAKURA** and RK4 have the largest dR .

We note that the magnitude of energy errors are not indicative of symplecticity. Two of the three methods with worst energy error, leapfrog and WHJ, are also two of the three methods that best conserve Poincaré invariants. By contrast, RK4 has a small energy error, similar to HB15's error, yet RK4 has the largest phase space volume element conservation error from all methods. Errors in first integrals do not indicate how well phase space volume elements are conserved.

Next we test the **MERCURY** switching integrator. We vary r_{crit} , which measures where in phase space the switch takes place. We calculate dR for each value of $c = r/r_{\text{crit}}$, where r

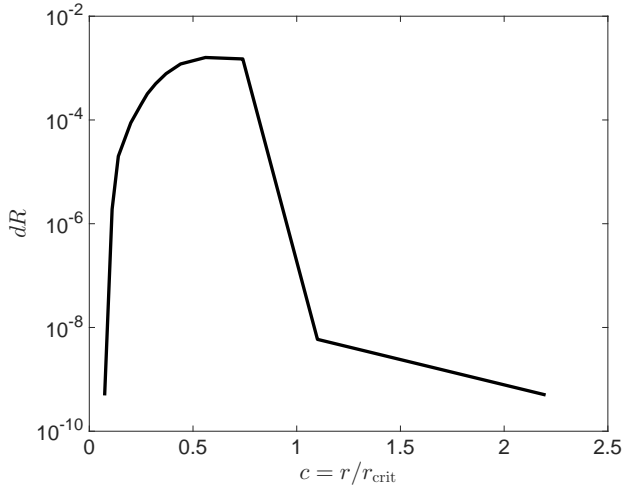


Figure 8. A measure of symplecticity for a phase space tube of MERCURY solutions of the binary planet hierarchical triple problem. $h = 0.001$ is used. The symplecticity deteriorates when c is in the range 0.1 to 1.

is the initial separation between the binary planets. Subject to other phase space coordinate requirements (Chambers 1999), for $c < 0.1$, MERCURY reduces to WHD. For $c > 1$, MERCURY reduces to BS, which we showed yields small dR . The result is shown in Fig. 8. We find the surprising result that phase space volume element conservation is strongly violated for some values of c . To try to understand why symplecticity is broken, we review how we calculated dR . For each Jacobian column we calculate, we run MERCURY 8 times. There are 12 columns corresponding to 12 phase space variables. A possible source of error is if during a number of the 96 MERCURY runs there were inconsistencies in the close encounter prescription. Another option is that there is a bug in the MERCURY code, but we could not find one. Thus, we find the surprising result of a violation in symplecticity of MERCURY. We did not have to search hard to find the violation.

4.4 Time Reversibility of MERCURY

Time reversibility, or time symmetry, is a highly desirable property of an integrator. Hairer, Lubich & Wanner (2006) show it can lead to benefits akin to symplecticity. To test reversibility of a method, we can run a method for time h and then for time $-h$. We should recover the initial conditions, neglecting roundoff error, regardless of the magnitude of h .

WHJ is reversible, as we can see by inspection and by numerical tests. We see by inspection that WHD is also reversible. Radau and BS are also approximately time symmetric in our tests. We test the reversibility of MERCURY by running forwards and backwards the hierarchical binary planet problem of Section 3.1 for several positive values of h and calculating the energy error. We try different values of r_{crit} . For reference, we also test HB15, which is a known reversible method.

The results are shown in Fig. 9. We plot reversibility curves for different values of the smoothing function K ,

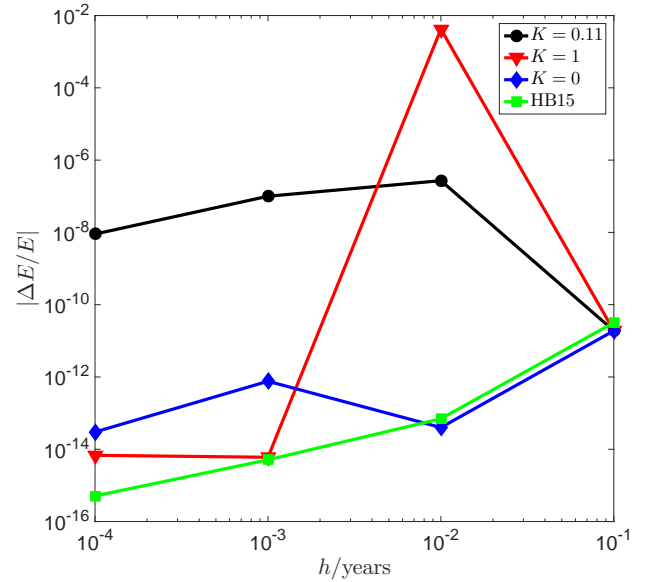


Figure 9. Time reversibility of MERCURY and HB15. A step forwards and then a step backwards of various sizes is taken when solving the hierarchical three body problem. Reversibility appears to especially break in the region where K is between 0 and 1, the black curve.

which ranges from 0 (Bulirsch Stoer) to 1 (WHD). We again input c (Section 4.3) into MERCURY and calculate K by using eq. 10 in Chambers (1999). All curves show breaks in reversibility; we must pick apart breaks due to roundoff or inherent to the methods. Errors in the HB15 curve grow with h and are due to roundoff error in operations like $d = e + hf$, with d, e , and f numbers. These operations result in greater losses of significant digits as h grows. The error of point $h = 0.01$ years for $K = 1$ appears not due to roundoff. The same holds for most of the curve $K = 0.11$. For possible explanations of the breaks, we offer the same possibilities that caused the break in symplecticity in Section 4.3. We also mention possible inaccuracies in the Kepler solver used by MERCURY. For more discussion on MERCURY's Kepler solver, see Wisdom & Hernandez (2015). Even though the two integrators of MERCURY used individually are time reversible, used in combination, in MERCURY, they are not.

4.5 Dynamically wrong results from MERCURY

Sections 4.2, 4.3, and 4.4 have highlighted concerns with switching integrators, focusing on MERCURY as an example. But it remains to be seen whether the problems have qualitative dynamical consequences. In this Section, we show an example where MERCURY gives dynamically incorrect results. The wrong results may be related to issues we presented or other bugs or problems we did not diagnose.

We again consider the binary planet problem. We increase the binary eccentricity to $e = 0.98$. The planet masses are each reduced by 10% to $8.9 \times 10^{-4} M_{\odot}$. We set $r_{\text{crit}} = 3r_{\text{Hill}}$ in an attempt to induce two switches per period P of the binary planet orbit near its periaapses: during its orbit, its c (Section 4.3) will range from 1.2×10^{-4} at apoapse to 0.12 at periaapses.

Table 2. Time of binary unbinding t_U of **MERCURY** for several time steps and tolerances. We did not find a set of parameters for which t_U was larger than 25 years. We also show the small energy error after 1000 years.

MERCURY			
h/P	Tol	t_U /years	$ \Delta E/E $
9.2×10^{-2}	1×10^{-12}	11	1.3×10^{-9}
9.2×10^{-3}	1×10^{-14}	25	1.9×10^{-9}
9.2×10^{-4}	1×10^{-11} and 1×10^{-12}	3.9	1.2×10^{-9}

Table 3. Time of binary unbinding t_U of HB15 for different time steps. We did not find time steps for which t_U was less than 1000 years.

HB15		
h/P	t_U /years	$ \Delta E/E $
9.2×10^{-3}	> 1000	3.5×10^{-4}
1.8×10^{-3}	> 1000	3.7×10^{-7}
9.2×10^{-4}	> 1000	4.5×10^{-10}

We run **MERCURY** and HB15 for 1,000 years with different step sizes and tolerances (Tol) and measure the energy error and the unbinding time t_U of the binary planet. We show results for **MERCURY** in Table 2 and results for HB15 in Table 3. The difference is that $t_U < 25$ years in all **MERCURY** runs, while $t_U > 1000$ years in all HB15 runs. We investigated a solution from the final row of Table 2 and found t_U corresponds approximately to a periaapses passage. Despite the small errors in energy and angular momentum (now shown) in **MERCURY**, we believe the correct t_U is given by the phase space volume conserving HB15 method.

The periodic behavior of the phase space coordinates suggests the HB15 solutions are approximately quasi-periodic for at least 1000 years, and the **MERCURY** solutions are approximately quasi-periodic until their time t_U . To study this, we focus attention on the $h/P = 9.2 \times 10^{-4}$ and Tol = 1×10^{-12} , for **MERCURY**, solutions. For one method at a time, we calculate the L_1 norm as a function of time between solutions in a phase space tube that have nearby initial conditions. L_1 as a function of time quantifies the divergence of the solutions. We find no clear evidence of exponential divergence, characteristic of chaotic dynamics, for the solution trajectories of either method. We then choose one of the 12 phase space coordinates, and plot it as a function of time for both HB15 and **MERCURY**, on the same graph. The y -axis scale is set by the maximum and minimum phase space coordinate values between time 0 and 3.9 years, **MERCURY**'s t_U . We find the HB15 and **MERCURY** trajectories are indistinguishable until time 3.9 years. We repeated the experiment for several phase space coordinates and the trajectories in time remained indistinguishable.

To confirm HB15's results for t_U , the same test was run with a different widely used integrator, not part

Table 4. Time of binary unbinding t_U of a time symmetric Hermite method for several values of η and number of iterations. No set of parameters were found for which t_U was less than 1000 years.

Hermite				
$< h > /P$	η	Max. Iter.	t_U /years	$ \Delta E/E $
3.2×10^{-3}	0.1	5	> 1000	4.8×10^{-4}
1.6×10^{-3}	0.05	3	> 1000	1.6×10^{-5}
3.1×10^{-4}	0.01	5	> 1000	8.0×10^{-9}

of the **MERCURY** software, the fourth order Hermite integrator with shared adaptive time steps, described in Kokubo, Yoshinaga & Makino (1998). The method is claimed to be approximately time symmetric for near constant time steps. In one comparison below, it is significantly slower than HB15. Different η (Aarseth, Tout & Mardling 2008, Chapter 1) and iteration numbers are set and the average h , $< h >$ is calculated. Some results are shown in Table 4.

t_U is again always > 1000 years. For $\eta = 0.05$, a precession in the orientation of the Runge-Lenz vector of the binary was measured with period of ≈ 329 years; a similar effect is seen when two body eccentric orbits are studied with leapfrog. Leapfrog shows precession because there is no nearby first integral to the argument of pericenter in the exact two-body leapfrog solution. The two-body leapfrog solution approximately conserves the actions, responsible for the solution topology, but has linear drift in the angles error. The third row of Table 4 took 6-10 times more computing effort than the third row of Table 3, despite the HB15 error being smaller: Hermite is not as efficient as HB15 for at least some of the parameter space.

As an additional check of the results of HB15 and Hermite, we solve the binary planet problem using the popular explicit 4th order method described in Yoshida (1990), which assumes the position and momentum dependence of the Hamiltonian is separable. The method conserves all first integrals of the N -body problem, except the energy, exactly. We use it with inertial Cartesian coordinates. The method is slow for the binary planet problem, but it is symplectic and time symmetric, and adequate for checking our solutions. We must use it with a small time step. We choose a step $h/P = 9.2 \times 10^{-5}$, 10 times smaller than the smallest step in Table 2. After 1000 years the binary was still bound and the energy error was $|\Delta E/E| = 1.7 \times 10^{-11}$.

As a final test a linear multistep method is used to find the solution of the binary planet problem. An Adams-Bashforth-Moulton predictor-corrector implicit method (Binney & Tremaine 2008) is used. An implicit method is well suited to solve the stiff system of ordinary differential equations associated with our hierarchical triple problem. In agreement with the HB15 solution, $t_U > 300$ years (computation was terminated at time 300 years) is found.

Thus, we have found without difficulty an N -body problem for which **MERCURY** predicts a binary will unbind, unphysically, despite **MERCURY**'s small errors in energy and angular

momentum. Several checks suggest the correct binary behavior is given by the HB15 solution. We remark that the Radau and BS methods in the **MERCURY** package also had $t_U < 50$ years.

5 CONCLUSIONS AND RECOMMENDATIONS

For years, switching methods have been popular methods for solving problems in solar system dynamics and formation. **MERCURY** is cited frequently and it is publicly available and easy to use. The first aim of this paper is to establish the validity and limitations of switching methods in general, and **MERCURY** in particular. We show that **MERCURY** can give dynamically incorrect results even when first integral errors are small. We have not proven the wrong solutions are due to a switch; in fact, the Radau and BS implementations in **MERCURY** also give erroneous solutions. We suggest caution must be exercised when using **MERCURY** and other switching methods, and their results should be checked using other methods.

We apply the exactly - ignoring roundoff and Kepler solver error- symplectic and reversible method of Hernandez & Bertschinger (2015) that uses intuitive inertial Cartesian coordinates to problems in solar system dynamics and offer it as an alternative to switching methods. For adequate time steps, it was able to integrate accurately every close encounter in its solutions. When compared against **MERCURY** and WHD without symplectic correctors, it is found to be highly efficient. Further efficiency tests were done in Hernandez & Bertschinger (2015). Its roundoff error behavior follows the Brownian motion described by Brouwer's law. We expect it may be more efficient than the code **IAS15** for long term problems, where statistical results of N -body integrations are most meaningful. The errors of HB15 can be reduced to the machine precision by using a symplectic corrector and its inverse at virtually no additional computational cost. We have not developed symplectic correctors here; because they will involve three, and not two, generally non-commuting operators, coefficient formulae in Wisdom (2006) do not apply.

HB15 is easy to implement and its steps are described partly in Algorithm 1. We recommend its use for solving general solar system dynamics problems including those with multiple stars, binary planets, or planets with satellites. HB15 can be used to check existing solutions from **MERCURY** or **IAS15**.

6 ACKNOWLEDGEMENTS

This work was begun after conversations with Piet Hut, Gerry Sussman, and Scott Tremaine. I appreciate feedback from Ed Bertschinger, Jack Wisdom, Scott Tremaine, and Katherine Deck. The results of the Hermite code were obtained by Kento Masada, and results of the Adams-Bashforth-Moulton method were obtained by Uchupol Ruangsri. I acknowledge support by the National Science Foundation Graduate Research Fellowship under Grant No. 1122374.

REFERENCES

- Aarseth S. J., Tout C. A., Mardling R. A., eds., 2008, *Lecture Notes in Physics*, Berlin Springer Verlag, Vol. 760, The Cambridge N-Body Lectures. Springer Verlag, Berlin
- Antognini J. M. O., Thompson T. A., 2015, ArXiv e-prints
- Batygin K., Brown M. E., Betts H., 2012, *ApJL*, 744, L3
- Binney J., Tremaine S., 2008, *Galactic Dynamics: Second Edition*. Princeton University Press
- Brouwer D., 1937, *AJ*, 46, 149
- Chambers J. E., 1999, *MNRAS*, 304, 793
- Chambers J. E., Quintana E. V., Duncan M. J., Lissauer J. J., 2002, *AJ*, 123, 2884
- Chirikov B. V., 1979, *Physics Reports*, 52, 263
- Dragt A. J., Finn J. M., 1976, *Journal of Mathematical Physics*, 17, 2215
- Duncan M. J., Levison H. F., Lee M. H., 1998, *AJ*, 116, 2067
- Gonçalves Ferrari G., Boekholt T., Portegies Zwart S. F., 2014, *MNRAS*, 440, 719
- Gustafson J. L., 2015, *The End of Error: Unum Computing*. Chapman and Hall/CRC
- Hairer E., Lubich C., Wanner G., 2006, *Geometrical Numerical Integration*, 2nd edn. Springer Verlag, Berlin
- Hairer E., McLachlan R., Razakarivony A., 2008, *BIT*, 48, 231
- Heggie D., Hut P., 2003, *The Gravitational Million-Body Problem: A Multidisciplinary Approach to Star Cluster Dynamics*. Cambridge University Press
- Hernandez D. M., Bertschinger E., 2015, *MNRAS*, 452, 1934
- Horch E. P., Howell S. B., Everett M. E., Ciardi D. R., 2014, *ApJ*, 795, 60
- Iwasawa M., Portegies Zwart S., Makino J., 2015, *Computational Astrophysics and Cosmology*, 2, 6
- Kokubo E., Yoshinaga K., Makino J., 1998, *MNRAS*, 297, 1067
- Kvaerno A., Leimkuhler B., 2000, *SIAM J. Sci. Comp.*, 22, 1016
- Laskar J., Robutel P., Joutel F., Gastineau M., Correia A. C. M., Levrard B., 2004, *AAp*, 428, 261
- Lichtenberg A. J., Lieberman M. A., 1983, *Regular and stochastic motion*. Springer Verlag
- Oshino S., Funato Y., Makino J., 2011, *PASJ*, 63, 881
- Portegies Zwart S., Boekholt T., 2014, *ApJ*, 785, L3
- Quinlan G. D., Tremaine S., 1992, *MNRAS*, 259, 505
- Rein H., Spiegel D. S., 2015, *MNRAS*, 446, 1424
- Rein H., Tamayo D., 2015, *MNRAS*, 452, 376
- Sanz-Serna J., Calvo M., 1994, *Numerical Hamiltonian Problems*, 1st edn. Chapman and Hall, London
- Springel V., 2005, *MNRAS*, 364, 1105
- Sussman G. J., Wisdom J., 2001, *Structure and interpretation of classical mechanics*. The MIT Press
- Wisdom J., 2006, *AJ*, 131, 2294
- Wisdom J., Hernandez D. M., 2015, *MNRAS*, 453, 3015
- Wisdom J., Holman M., 1991, *AJ*, 102, 1528
- Wisdom J., Holman M., Touma J., 1996, *Fields Institute Communications*, Vol. 10, p. 217, 10, 217
- Yoshida H., 1990, *Physics Letters A*, 150, 262
- Yoshida H., 1993, *Celest. Mech. Dyn. Astron.*, 56, 27
- Zhong G., Marsden J. E., 1988, *Physics Letters A*, 133, 134